

Ab initio calculation of the Transmission Coefficients from a Superlattice electronic structure

Ingmar Riedel, Peter Zahn, and Ingrid Mertig
Institut für Theoretische Physik
Technische Universität Dresden, D-01062 Dresden, Germany
(November 19, 2018)

arXiv:cond-mat/0011059v1 [cond-mat.mtrl-sci] 3 Nov 2000

Typeset using REVTeX

Abstract

A new formalism to calculate the transmission coefficient t of electrons from a material \mathcal{L} into the same material \mathcal{L} through a barrier \mathcal{B} is presented. The barrier \mathcal{B} is arbitrary and can be metallic, semiconducting or insulating. The important feature of this formalism is that it starts from the electronic structure of a periodic \mathcal{L}/\mathcal{B} superlattice. The electronic structure of such a superlattice is calculated selfconsistently within a Screened Korringa-Kohn-Rostoker method. The capability of the new method is demonstrated by means of a free electron model. First results for the transmission of Cu electrons through a Co layer are presented.

I. INTRODUCTION

If Bloch electrons encounter planar interfaces they may be reflected or transmitted. In this paper we develop a technique for the calculation of these reflection and transmission amplitudes within the Screened Korringa-Kohn-Rostoker (Screened KKR) approach, a technique for ab initio electronic structure calculations.

There are many uses for Bloch wave transmission and reflection amplitudes and probabilities. First of all they can be applied to describe transport [1,2] in films and multilayers including the electronic structure of the real material. Secondly, they can be used to develop a first principle based theory of electron tunneling. Finally, transmission and reflection coefficients are the basic ingredients for the theoretical understanding of interlayer exchange coupling [3].

Consider an arbitrary barrier \mathcal{B} which is sandwiched by two leads of the material \mathcal{L} (see Fig. 1). For the propagating bulk-states in \mathcal{L} the transmission coefficient t through the barrier is defined as

$$t = \frac{A_1}{A_0} \text{ for } B_1 = 0 \quad (1)$$

where the $A_{0,1}$ and B_1 are the complex amplitudes of the right- and left-moving Bloch waves. During the scattering process the energy E and the in-plane component \mathbf{k}_{\parallel} of the wave vector ($k, \mathbf{k}_{\parallel}$) are conserved.

In the past different methods were established for the calculation of t , e.g. [4–6]. These methods usually model the structure of the two semi-infinite leads \mathcal{L} separated by a barrier \mathcal{B} . Via the Green's function or the wave function of the system t can be computed. In this work we present a new method which approaches the problem differently: We use the band structure and wave function of a periodic superlattice \mathcal{B}/\mathcal{L} to calculate t . This is strongly motivated by the development of highly efficient N-scaling superlattice KKR codes, e.g. [7–10].

A superlattice is a structure \mathcal{B}/\mathcal{L} which is periodically repeated in all three dimensions (see Fig. 2). Therefore the case of the single barrier \mathcal{B} with leads \mathcal{L} is fully contained in this structure and the similarity with the Kronig-Penney model is obvious. Kronig and Penney showed in their simple 1-dimensional free electron model how the bandstructure of a periodic

system can be derived from the scattering properties of a single barrier. (For more details on the Kronig-Penney model see for instance [11].)

The keynote of this paper is to derive the scattering properties of a single barrier from the electronic structure of a superlattice. We discuss the theory and numerical implementation of the new method and present its first successful applications to free electrons and a Cu/Co (001) system.

II. THEORY

First we state our basic assumptions. Thereafter we discuss the transmission coefficient t of the single barrier and finally its connection to the superlattice wave function.

A. Basic assumptions

In Fig. 1 and Fig. 2 schematic pictures of a single barrier and a superlattice are presented. Note that x is always perpendicular to the barrier \mathcal{B} , the other two components are denoted with \mathbf{r}_{\parallel} . Along \mathbf{r}_{\parallel} the leads \mathcal{L} and the barrier \mathcal{B} show the same 2-dimensional periodicity. The superlattice, however, is also periodic in x -direction.

The single barrier case (see Fig. 1) consists of the barrier and two semi-infinite leads. In difference to the common understanding, we will include the perturbed interface regions of the leads into the barrier \mathcal{B} . The leads \mathcal{L} , however, consist of bulk-like potentials only. A superlattice (see Fig. 2) consists of an infinite number of barriers separated by interlayers. The barriers \mathcal{B} contain again the perturbed interface regions. The interlayers consist of bulk-like potentials, the same as in the leads \mathcal{L} of the single barrier case.

Furthermore, we assume energy- and \mathbf{k}_{\parallel} -conservation due to the elastic scattering and the in-plane symmetry of the system. Since \mathbf{k}_{\parallel} is conserved the problem can be treated as quasi 1-dimensional, but the reader should be cautious while keeping track of the components of the other two dimensions.

We make two additional simplifications: First, the barrier is symmetric and, secondly, we restrict our considerations to one propagating bulk state $\Phi^{(k, \mathbf{k}_{\parallel})}(x, \mathbf{r}_{\parallel})$ at a given energy and \mathbf{k}_{\parallel} . That means, degeneration and band-crossing of bulk states in the leads are excluded.

B. The single barrier

The wavefunction in the leads \mathcal{L} is a superposition of the right- and left-moving bulk states, since the solution of the Schrödinger equation depends only on the local potential (see Fig. 1):

$$\Psi(x, \mathbf{r}_{\parallel}) = A_n e^{ikx} e^{i\mathbf{k}_{\parallel}\mathbf{r}_{\parallel}} u_{k, \mathbf{k}_{\parallel}}(x, \mathbf{r}_{\parallel}) + B_n e^{-ikx} e^{i\mathbf{k}_{\parallel}\mathbf{r}_{\parallel}} u_{-k, \mathbf{k}_{\parallel}}(x, \mathbf{r}_{\parallel}) . \quad (2)$$

$n = \{0, 1\}$ denotes the two sides of the barrier. $\Phi^{(k, \mathbf{k}_{\parallel})}(x, \mathbf{r}_{\parallel}) = e^{ikx} e^{i\mathbf{k}_{\parallel}\mathbf{r}_{\parallel}} u_{k, \mathbf{k}_{\parallel}}(x, \mathbf{r}_{\parallel})$ is the Bloch function of the bulk system. The decomposition of $\Phi^{(k, \mathbf{k}_{\parallel})}(x, \mathbf{r}_{\parallel})$ into a phase factor and a periodic function is due to Bloch's theorem with $u_{k, \mathbf{k}_{\parallel}}(x, \mathbf{r}_{\parallel}) = u_{k, \mathbf{k}_{\parallel}}(x - md, \mathbf{r}_{\parallel})$, where d is the bulk lattice parameter and m an integer.

The amplitudes A_n and B_n on both sides of the barrier are related to each other by a transfer matrix M which describes all the scattering processes inside the barrier:

$$\begin{pmatrix} A_0 \\ B_0 \end{pmatrix} = M \begin{pmatrix} A_1 \\ B_1 \end{pmatrix}. \quad (3)$$

The four complex variables of this M -matrix are not independent from each other. Due to time-reversal invariance, current conservation and the symmetry of the barrier, M can be parametrized with two independent real parameters α_1 and β_1 in the following form [11]:

$$M = \begin{pmatrix} \alpha_1 + i\beta_1 & i\beta_2 \\ -i\beta_2 & \alpha_1 - i\beta_1 \end{pmatrix} \quad (4)$$

with $\beta_2^2 = \alpha_1^2 + \beta_1^2 - 1$.

Therefore the relation $M^{-1} = M^*$ is valid.

Using the components of the transfer matrix the transmission coefficient t is by definition Eq. (1):

$$t = \frac{1}{\alpha_1 + i\beta_1}. \quad (5)$$

Obviously, the problem is solved if the eigenstates $\Psi(x, \mathbf{r}_{\parallel})$ of such a single barrier are known.

C. The superlattice

In contrast to the eigenfunctions of the single barrier (see Eq. (2)) the eigenfunctions of a superlattice $\Psi(x, \mathbf{r}_{\parallel})$ are described by quantum numbers $(\kappa, \mathbf{k}_{\parallel})$. Here, κ is the superlattice wave vector in x -direction reflecting the prolonged lattice structure with the lattice constant l , that is the length of the unit cell in x -direction. Furthermore, the in-plane component \mathbf{k}_{\parallel} is the same as in the bulk system since in-plane symmetry is conserved. The translational symmetry of $\Psi^{(\kappa, \mathbf{k}_{\parallel})}$ in the superlattice direction is given by Bloch's theorem:

$$\Psi^{(\kappa, \mathbf{k}_{\parallel})}(x, \mathbf{r}_{\parallel}) = \left(e^{-i\kappa l}\right)^n \Psi^{(\kappa, \mathbf{k}_{\parallel})}(x + nl, \mathbf{r}_{\parallel}), \quad (6)$$

where the integer n ranges from minus to plus infinity.

Let us now consider the superlattice as a periodic repetition of single barriers \mathcal{B} with the interlayer \mathcal{L} in between. In the interlayer the potential is bulk-like and therefore we can expand the superlattice wave function (see Eq. (6)) as a superposition of right- and left-moving Bloch functions of the bulk system in the cell $n = 0$ ($a \leq x \leq a + s$):

$$\begin{aligned} & A_0 e^{ikx} e^{i\mathbf{k}_{\parallel} \mathbf{r}_{\parallel}} u_{k, \mathbf{k}_{\parallel}}(x, \mathbf{r}_{\parallel}) + B_0 e^{-ikx} e^{i\mathbf{k}_{\parallel} \mathbf{r}_{\parallel}} u_{-k, \mathbf{k}_{\parallel}}(x, \mathbf{r}_{\parallel}) \\ & = \left(e^{-i\kappa l}\right)^n \left[A_n e^{ik(x+nl)} e^{i\mathbf{k}_{\parallel} \mathbf{r}_{\parallel}} u_{k, \mathbf{k}_{\parallel}}(x + nl, \mathbf{r}_{\parallel}) + B_n e^{-ik(x+nl)} e^{i\mathbf{k}_{\parallel} \mathbf{r}_{\parallel}} u_{-k, \mathbf{k}_{\parallel}}(x + nl, \mathbf{r}_{\parallel}) \right]. \end{aligned} \quad (7)$$

By using the relation $u_{k, \mathbf{k}_{\parallel}}(x + nl, \mathbf{r}_{\parallel}) = u_{k, \mathbf{k}_{\parallel}}(x, \mathbf{r}_{\parallel})$ we can rewrite this into

$$A_0 e^{ikx} e^{i\mathbf{k}_\parallel \mathbf{r}_\parallel} u_{k, \mathbf{k}_\parallel}(x, \mathbf{r}_\parallel) + B_0 e^{-ikx} e^{i\mathbf{k}_\parallel \mathbf{r}_\parallel} u_{-k, \mathbf{k}_\parallel}(x, \mathbf{r}_\parallel) \quad (8)$$

$$= (e^{-i\kappa l})^n \left[A_n e^{iknl} e^{ikx} e^{i\mathbf{k}_\parallel \mathbf{r}_\parallel} u_{k, \mathbf{k}_\parallel}(x, \mathbf{r}_\parallel) + B_n e^{-iknl} e^{-ikx} e^{i\mathbf{k}_\parallel \mathbf{r}_\parallel} u_{-k, \mathbf{k}_\parallel}(x, \mathbf{r}_\parallel) \right]. \quad (9)$$

Since the right- and left-moving bulk states are orthogonal we find

$$\begin{pmatrix} A_0 \\ B_0 \end{pmatrix} = (e^{-i\kappa l})^n \begin{pmatrix} A_n e^{iknl} \\ B_n e^{-iknl} \end{pmatrix}. \quad (10)$$

On the other hand we can connect the amplitudes in different cells with the transfer matrix M :

$$\begin{pmatrix} A_0 \\ B_0 \end{pmatrix} = M^n \begin{pmatrix} A_n \\ B_n \end{pmatrix}. \quad (11)$$

We can combine Eqs. (10) and (11) to the eigenvalue equation

$$e^{i\kappa l} \begin{pmatrix} A_0 \\ B_0 \end{pmatrix} = P \begin{pmatrix} A_0 \\ B_0 \end{pmatrix} \quad (12)$$

with

$$P = \begin{pmatrix} e^{ikl} & 0 \\ 0 & e^{-ikl} \end{pmatrix} M^{-1} \quad (13)$$

$$= \begin{pmatrix} (\alpha_1 - i\beta_1)e^{ikl} & -i\beta_2 e^{ikl} \\ i\beta_2 e^{-ikl} & (\alpha_1 + i\beta_1)e^{-ikl} \end{pmatrix}. \quad (14)$$

Since P is fully determined by the single eigenvalue $e^{i\kappa l}$ and the corresponding eigenvector $\begin{pmatrix} A_0 \\ B_0 \end{pmatrix}$, we obtain the following algebraic set for α_1 and β_1 :

$$\begin{aligned} \beta_2^2 &= \alpha_1^2 + \beta_1^2 - 1 \\ \frac{A_0}{B_0} &= \frac{\beta_2 e^{ikl}}{\alpha_1 \sin kl - \beta_1 \cos kl - \sin \kappa l} \\ \cos \kappa l &= \alpha_1 \cos kl + \beta_1 \sin kl. \end{aligned} \quad (15)$$

Thus, we are able to calculate t for a given energy and \mathbf{k}_\parallel knowing k , κ and $\frac{A_0}{B_0}$ of the superlattice wave function $\Psi^{(\kappa, \mathbf{k}_\parallel)}$ and corresponding bulk state $\Phi^{(k, \mathbf{k}_\parallel)}$.

III. NUMERICAL ASPECTS

In this section we explain how to extract k and $\frac{A_0}{B_0}$ from $\Psi^{(\kappa, \mathbf{k}_\parallel)}(x, \mathbf{r}_\parallel)$ in the interlayer, which is very similar to a Fourier analysis of the $\Psi^{(\kappa, \mathbf{k}_\parallel)}(x, \mathbf{r}_\parallel)$. For the electronic band structure calculations we used a Screened Korrington-Kohn-Rostoker (Screened KKR) method.

A. Brief introduction to the Screened KKR method

The Screened KKR method (see [7–10]) was developed for the selfconsistent calculation of the electronic structure. It is based on Green's functions and the computation time scales linearly with the number of atoms in the unit cell. This allows the computation of systems with a relatively large number of atoms. For the atomic potentials the atomic sphere approximation (ASA) is used. The superlattice wave function is expanded in terms of spherical solutions:

$$\Psi^\kappa(\mathbf{R}^n + \mathbf{r}_\mu + \mathbf{r}) = \sum_L e^{i\kappa\mathbf{R}^n} C_L^\mu(\kappa) R_l^\mu(r, E) Y_L(\hat{r}), \quad (16)$$

the wave function in the leads as well:

$$\Phi^{\mathbf{k}}(\mathbf{R}^n + \mathbf{r}_\mu + \mathbf{r}) = \sum_L e^{i\mathbf{k}\mathbf{R}^n} \hat{C}_L^\mu(\mathbf{k}) R_l^\mu(r, E) Y_L(\hat{r}). \quad (17)$$

\mathbf{R}^n is the lattice vector pointing to the n^{th} unit cell, \mathbf{r}_μ refers to the μ^{th} atom in the unit cell and \mathbf{r} is the space coordinate inside the μ^{th} atomic sphere. The $Y_L(\hat{r})$ are the spherical harmonics with the short hand notation $L = (l, m)$, l is the angular momentum and m the magnetic quantum number. $R_l^\mu(r, E)$ is the radial solution of the Schrödinger equation in the μ^{th} atomic sphere. The $C_L^\mu(\kappa)$ and $\hat{C}_L^\mu(\mathbf{k})$ are the expansion coefficients, $\kappa = (\kappa, \mathbf{k}_\parallel)$ and $\mathbf{k} = (k, \mathbf{k}_\parallel)$ are the Bloch vectors in the superlattice and in the bulk system, respectively.

Angular momenta up to $l_{\text{max}} = 3$ were taken into account.

B. Implementation

As already explained, the superlattice wave function $\Psi^{(\kappa, \mathbf{k}_\parallel)}$ in the interlayer \mathcal{L} can be decomposed in right- and left-moving Bloch waves $\Phi^{(k, \mathbf{k}_\parallel)}$ and $\Phi^{(-k, \mathbf{k}_\parallel)}$:

$$\Psi^{(\kappa, \mathbf{k}_\parallel)} = A_0 \Phi^{(k, \mathbf{k}_\parallel)} + B_0 \Phi^{(-k, \mathbf{k}_\parallel)}. \quad (18)$$

Using the angular momentum expansions of Eqs. (16) and (17) we can expand Eq. (18) in the 0^{th} unit cell, which corresponds to $\mathbf{R}^0 = (-l, 0, 0)$:

$$\begin{aligned} & \sum_L e^{-i\kappa l} C_L^\mu(\kappa, \mathbf{k}_\parallel) R_l^\mu(r, E) Y_L(\hat{r}) \\ &= \sum_L \left[\begin{array}{l} A_0 e^{-ikl} \hat{C}_L^\mu(k, \mathbf{k}_\parallel) R_l^\mu(r, E) Y_L(\hat{r}) \\ + B_0 e^{ikl} \hat{C}_L^\mu(-k, \mathbf{k}_\parallel) R_l^\mu(r, E) Y_L(\hat{r}) \end{array} \right]. \end{aligned} \quad (19)$$

Now we make use of the orthogonality relation of the $Y_L(\hat{r})$ and the following relations between the $\hat{C}_L^\mu(\pm k, \mathbf{k}_\parallel)$ due to the real potential of the leads and Bloch's theorem:

$$\hat{C}_L^\mu(\pm k, \mathbf{k}_\parallel) = e^{i(\pm k, \mathbf{k}_\parallel)(r_\mu - r_0)} \hat{C}_L^0(\pm k, \mathbf{k}_\parallel) \quad (20)$$

$$\hat{C}_L^0(-k, \mathbf{k}_\parallel) = (-1)^{l+m} \hat{C}_L^0(k, \mathbf{k}_\parallel). \quad (21)$$

So finally we conclude:

$$\begin{aligned}
0 = & e^{-i\kappa l} C_L^\mu(\kappa, \mathbf{k}_\parallel) \\
& - A_0 e^{-ikl} e^{i(k, \mathbf{k}_\parallel)(r_\mu - \mathbf{r}_0)} \widehat{C}_L^0(k, \mathbf{k}_\parallel) \\
& - B_0 e^{ikl} e^{i(-k, \mathbf{k}_\parallel)(r_\mu - \mathbf{r}_0)} \widehat{C}_L^0(k, \mathbf{k}_\parallel) (-1)^{l+m} .
\end{aligned} \tag{22}$$

We can exploit this equation at three different atomic positions μ in the interlayer and receive an algebraic set for k and the ratio $\frac{A_0}{B_0}$. It turns out that the $\widehat{C}_L^0(k, \mathbf{k}_\parallel)$ cancel, so no additional computation of the bulk eigenstates of the leads is necessary. All we have to compute are the eigenstates of the superlattice $\Psi^{(\kappa, \mathbf{k}_\parallel)}(x, \mathbf{r}_\parallel)$ for a given energy E and in-plane wave vector \mathbf{k}_\parallel which gives us the $C_L^\mu(\kappa, \mathbf{k}_\parallel)$ and κ . From here on we can calculate t via Eqs. (15) and (22). As a side effect we obtain the bandstructure $k(E)$ of the lead material. This gives us the nice opportunity for an intermediate test of our method as we will see in the next section.

Still there is another problem we are faced with: If κ is complex the corresponding $\Psi^{(\kappa, \mathbf{k}_\parallel)}(x, \mathbf{r}_\parallel)$ is evanescent which means it does not exist in the superlattice. In other words we are in a superlattice bandgap. But also in this energy range we want to calculate the corresponding k and t . One opportunity is the computation of the complex bandstructure and developing a similar formalism as the one described above. But usually the complex bandstructure is not available. Another nice idea is to vary the interlayer thickness $s = (l - 2a)$ (see Fig. 2): The superlattice bandstructure gets stretched or squeezed on the energy axis comparable to the eigenstates of a square well. In this way we can scan the whole energy range, albeit it makes more than one superlattice calculation necessary. We followed this second idea.

IV. RESULTS

The results we discuss in this section demonstrate that our new method is working successfully. We considered the scattering of free electrons through a rectangular barrier, which is analytically solvable. Furthermore we investigated the transmission of Cu electrons through 5 monolayers (ML) Co (001), which we compared with the results of Wildberger [12], who developed a different method for the computation of t . In addition to the $|t|(E)$ -dependence we checked the dispersion relation $k(E)$ of the lead material.

A. Free electrons through a rectangular barrier

Outside the barrier we modelled an exact free electron gas with constant potential $V = 0$. The barrier itself consists of five layers with muffin tin (MT) spheres of a constant potential inside the sphere. The potential height is $V = 0.125Ryd$ and they are arranged in an fcc lattice with a lattice constant of $d = 6.76a.u.$. This is only an approximate rectangular barrier, but the best one possible with ASA potentials.

In Fig. 3 the dependence of $|t|$ on $(E - \mathbf{k}_\parallel^2)$ for $\mathbf{k}_\parallel = \left(\frac{\pi}{2d}, \frac{\pi}{2d}\right)$ is plotted. The analytical curve was fitted to the numerical data with a potential height of the rectangular barrier $V = 0.76 \cdot 0.125Ryd$. This potential height is given by the dashed line. The factor 0.76 is very close to 0.74 which is the effective space filling of MT spheres on an fcc lattice. The remaining small difference of 0.02 and also the subtle deviations in the $|t|(E)$ -dependence can

be understood very well in terms of the different barrier shapes. The two numerical curves with the different interlayer thicknesses (circle and plus) coincide, which is a brilliant test for the validity of the method itself. The discontinuity of the curves is due to the superlattice bandgaps. Obviously these gaps can be filled with different interlayer thicknesses s . To fill all gaps more calculations with different interlayer thicknesses s would be necessary. This is not done here since we just want to demonstrate the capability of our new method. For a short interpretation we notice that the electrons have a low transmission coefficient below the barrier since they have to tunnel through. Above the barrier height they approach $t = 1$ very rapidly, the oscillations are due to interference effects on the barrier interfaces.

In Fig. 4 we show the correspondence between the calculated dependence of k on $(E - \mathbf{k}_{\parallel}^2)$ for different \mathbf{k}_{\parallel} (circle, cross and triangle) and the expected free electron dispersion (solid line), and obtain a very good agreement.

B. Cu electrons through 5 ML of Co (001)

We arranged the Co and Cu on a fcc lattice with a lattice constant of $6.76a.u.$. The value is larger than that of magnetic fcc Co and smaller than that of fcc Cu. The Co layer consists of 5 ML. The potentials of the Co layer and three Cu layers at both sides of the barrier are taken from a self-consistent Co_5Cu_7 supercell calculation and form the barrier \mathcal{B} . The potential in the middle of the Cu layer is a bulk-like Cu ASA potential. This approximation has no influence on the results and has the advantage that we can construct easily any Cu interlayer thickness s without doing an extra selfconsistent calculation.

Figure 5b and 5d show the $|t|(E)$ -dependence for $\mathbf{k}_{\parallel} = 0$ in the majority and minority channels. Since Co is a ferromagnetic material the superlattice bandstructure of Cu/Co has no more spin-degeneracy and we obtain spin-split majority and minority bands. As for the free electron results the curves for different interlayer thicknesses s match, which is not shown explicitly here. Large parts of the $|t|(E)$ -curve can be justified qualitatively by the band structure (BS) of Co and Cu, which are plotted in Fig. 5a (Co majority BS), Fig. 5c (Cu BS) and Fig. 5e (Co minority BS). First we discuss the $|t|(E)$ -dependence in the majority channel (see Fig. 5b):

Since the Co and Cu states have the same symmetry character in the energy region **I** the Cu electrons can propagate through the barrier very well, below the bottom of the Co band they have to tunnel. Therefore the behavior in section **I** is very similar to the free electron result as discussed in the previous subsection. In region **II** there are no propagating Cu bulk states and consequently there is no t . In region **III** we see that t is almost free electron like again, the rapid breakdown at about 0.45 Ryd corresponds the change of the symmetry character in the Co bands. Region **IV** has to be excluded from our discussion since the Cu band structure is degenerated there and hence our method is not applicable. In region **V**, including the Fermi level at 0.68Ryd , we obtain a t of almost 1 which is due to the corresponding band symmetries in Co and Cu.

In the minority channel (see Fig. 5d) we see two major differences to the majority channel in region **III** and **V**: In region **III** t is almost zero since the Co minority band has a gap there and so no band matching is possible between the Cu and Co states. In region **V** we see a low t below 0.64 Ryd. This is due to the upward shifted Co bands in comparison to the

majority channel and therefore no band matching between states with the same symmetry character occurs.

Furthermore, we compare our results in the energy region **V** (see Fig. 6a) with the results obtained with a different method by Wildberger [12] (see Fig. 6b), who used a semi-infinite structure with two Co barriers at a certain distance (which is comparable to our interlayer thickness s) for the calculation of the reflection coefficient $|r|$. The reflection coefficient $|r|$ is related to $|t|$ by $|r| = \sqrt{1 - |t|^2}$. In Fig. 6b we see their $|r|(E)$ -dependence for the majority- and minority-channel (dashed and solid line) for $\mathbf{k}_{\parallel} = 0$ around the Fermi energy. The agreement with our own results shown in Fig. 6a is very good. Slight differences are related to the different lattice parameters which were used. In addition, Wildberger evaluates the Green's function of the system for energies with a small imaginary part, which causes a broadening corresponding to a finite temperature. The agreement between our calculation and the calculation of Wildberger is a confirmation of the capability and the validity of our new method.

In Fig. 7 we see the band structure of fcc Cu along the line $\Gamma - X$. The solid line is taken from a pure Cu band structure calculation, the crosses denote the band structure $k(E)$ extracted from the superlattice calculation. The region between the dashed lines corresponds to region **IV** in Fig. 5 and has to be excluded for the reasons mentioned above. Again, the correspondence between both curves is perfect.

V. SUMMARY

We presented a new method to calculate the transmission coefficient t of bulk states through a single barrier from a superlattice band structure. Its validity is fully confirmed by the successful test results. At this state the method is restricted to symmetric barriers and to only one propagating bulk state at a given energy and in plane wave vector. The generalization to the case of more than one propagating bulk state and unsymmetric barriers is under development.

VI. ACKNOWLEDGMENT

We like to thank J. Opitz, J. Binder, M. Turek, W. John (TU Dresden), the group of G.E.W. Bauer (TU Delft) and the group of P.H. Dederichs (Forschungszentrum Jülich) for helpful discussions.

REFERENCES

- [1] R. Landauer, *Phil. Mag.* **21**, 863 (1970).
- [2] D. S. Fisher and P. A. Lee, *Phys. Rev. B* **23**, 6851 (1981).
- [3] P. Bruno, *Phys. Rev. B* **52**, 411 (1995).
- [4] M.D. Stiles, *J. Appl. Phys.* **79**, 5805 (1996).
- [5] J.M. MacLaren, X.G. Zhang, W.H. Butler, and X. Wang, *Phys. Rev. B* **59**, 5470 (1999).
- [6] K. Wildberger, R. Zeller, P.H. Dederichs, J. Kudrnovský, and P. Weinberger, *Phys. Rev. B* **58**, 13721 (1998).
- [7] R. Zeller, P.H. Dederichs, B. Újfalussy, L. Szunyogh, and P. Weinberger, *Phys. Rev. B* **52**, 8807 (1995).
- [8] P. Zahn, I. Mertig, R. Zeller, and P.H. Dederichs, *Proc. Mat. Res. Soc.* **475**, 525 (1997).
- [9] O.K. Anderson and O. Jepsen, *Phys. Rev. Lett.* **53**, 2571 (1984).
- [10] L. Szunyogh, B. Újfalussy, P. Weinberger, and J. Kollár, *Phys. Rev. B* **49**, 2721 (1994).
- [11] E. Merzbacher, in *Quantum Mechanics*, Second Edition, John Wiley & Sons, New York (1970).
- [12] K. Wildberger, Ph.D. Thesis, *Tight-Binding-Korringa-Kohn-Rostoker-Methode und Grenzflächenreflektivität in magnetischen Schichtsystemen*, RWTH Aachen (1997).

FIGURES

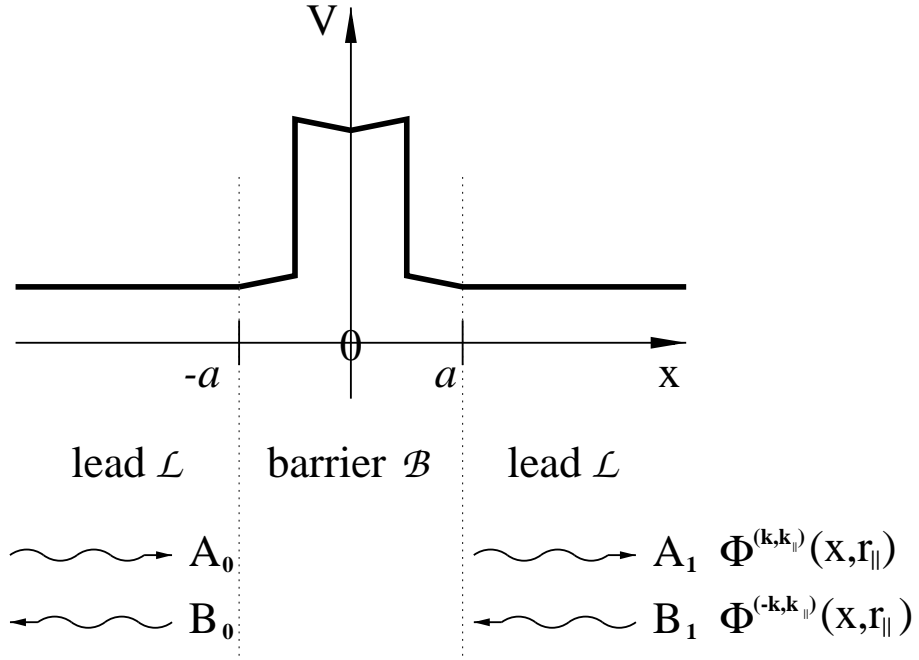


FIG. 1. Schematic drawing of the single barrier case with a barrier \mathcal{B} (including the perturbed interface regions) and leads \mathcal{L} . Furthermore, right- and left-moving eigenstates Φ are shown.

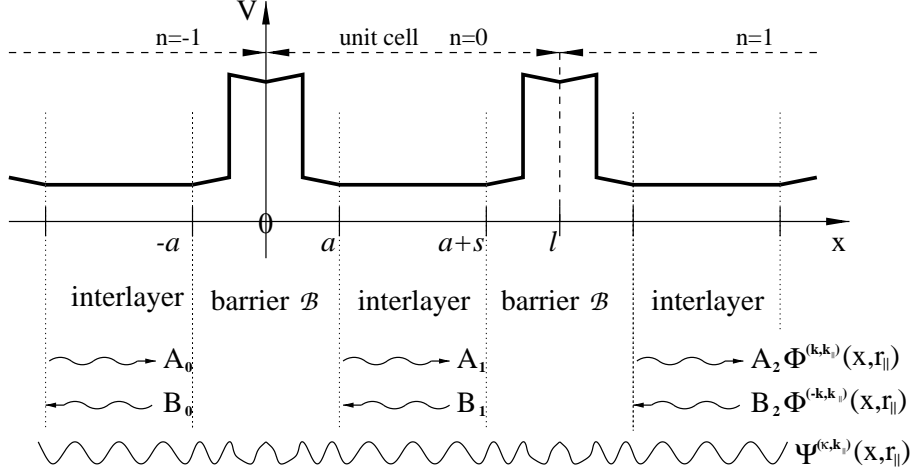


FIG. 2. Schematic drawing of the superlattice with barriers \mathcal{B} (including the perturbed interface regions) and interlayer \mathcal{L} . The superlattice wave function Ψ in the interlayers is a superposition of right- and left-moving bulk eigenstates Φ .

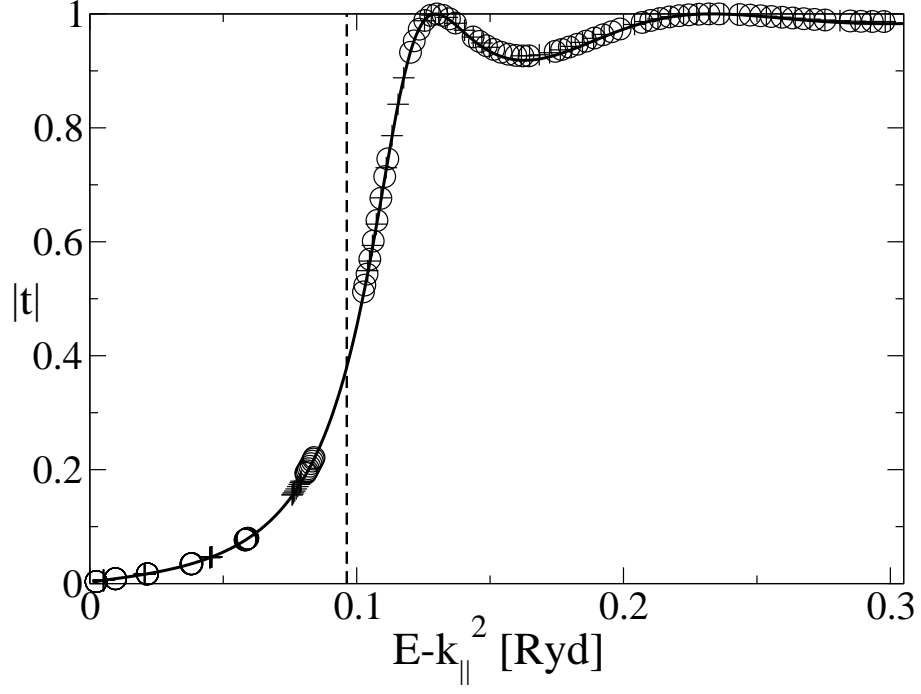


FIG. 3. The dependence of $|t|$ on $(E - \mathbf{k}_{\parallel}^2)$ for $\mathbf{k}_{\parallel} = (\frac{\pi}{2d}, \frac{\pi}{2d})$ of free electrons through a rectangular barrier with a thickness of 5 ML and an averaged height of 0.092 Ryd denoted by the dashed line: Analytical results (solid line) in comparison with the results obtained with our new method for two different interlayer thicknesses (cross: 11 ML, circle: 17 ML).

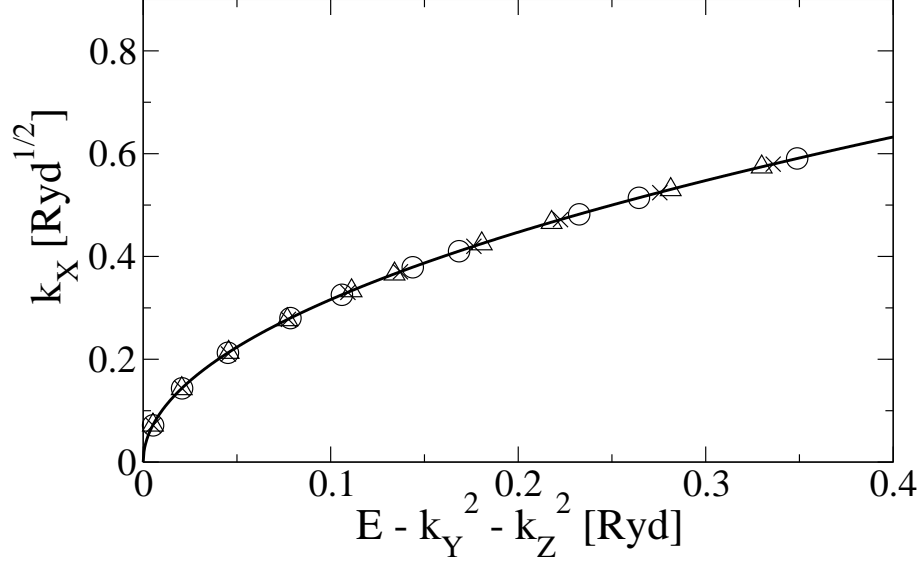


FIG. 4. The dispersion relation of free electrons for different \mathbf{k}_{\parallel} (circle: $k_x = k_y = 0$, cross: $k_x = 0.5, k_y = 0$; triangle: $k_x = k_y = 0.5$, all in relative units of the Brillouin zone) in comparison with the analytical result (solid line).

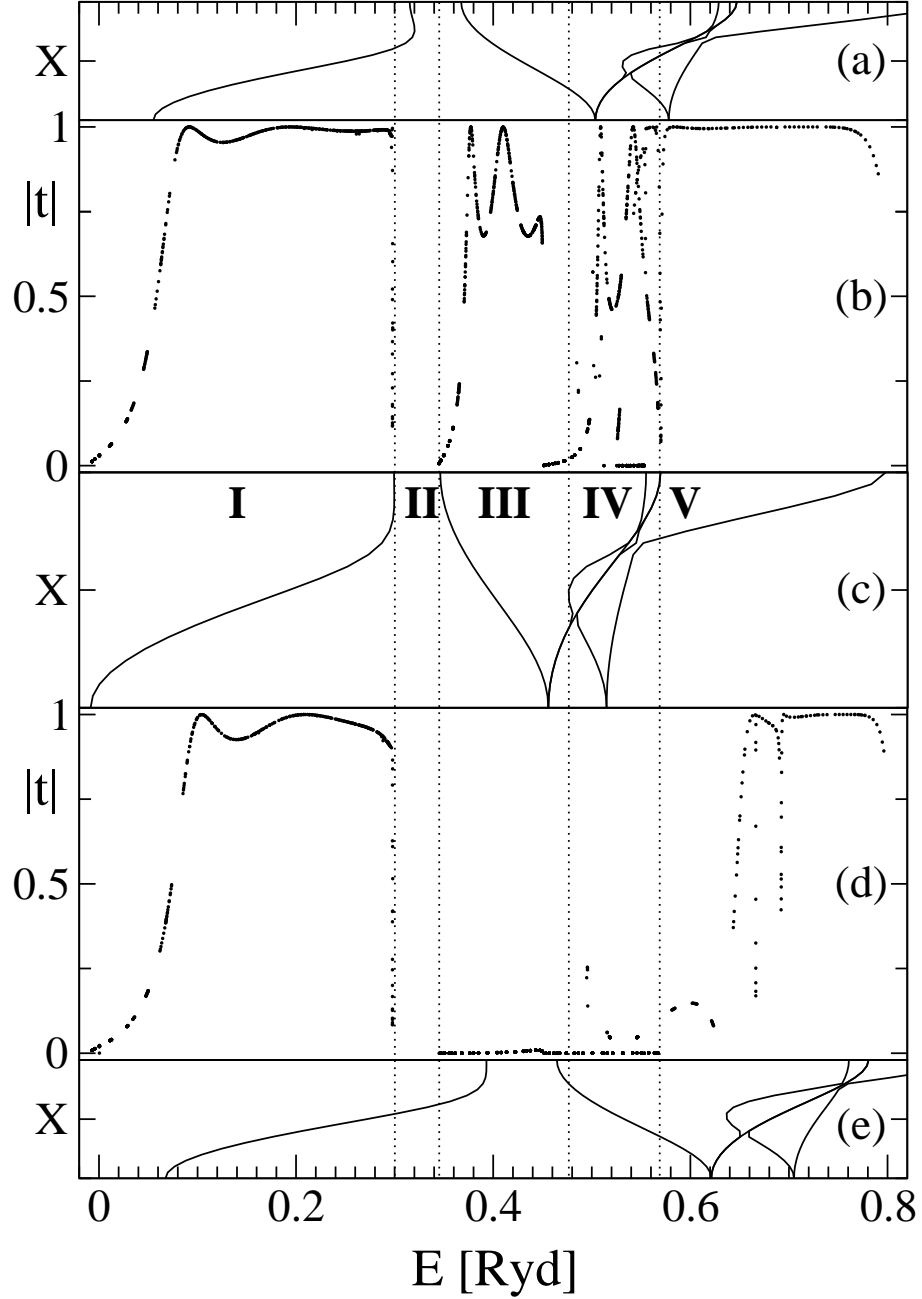


FIG. 5. Band structure of the majority (a) and minority (e) electrons of Co, band structure of Cu (c), furthermore the $|t|(E)$ -dependence for Cu electrons through the majority (b) and minority (d) potential barrier of 5 ML Co; all along the line $\Gamma - X$, that is $\mathbf{k}_{\parallel} = 0$.

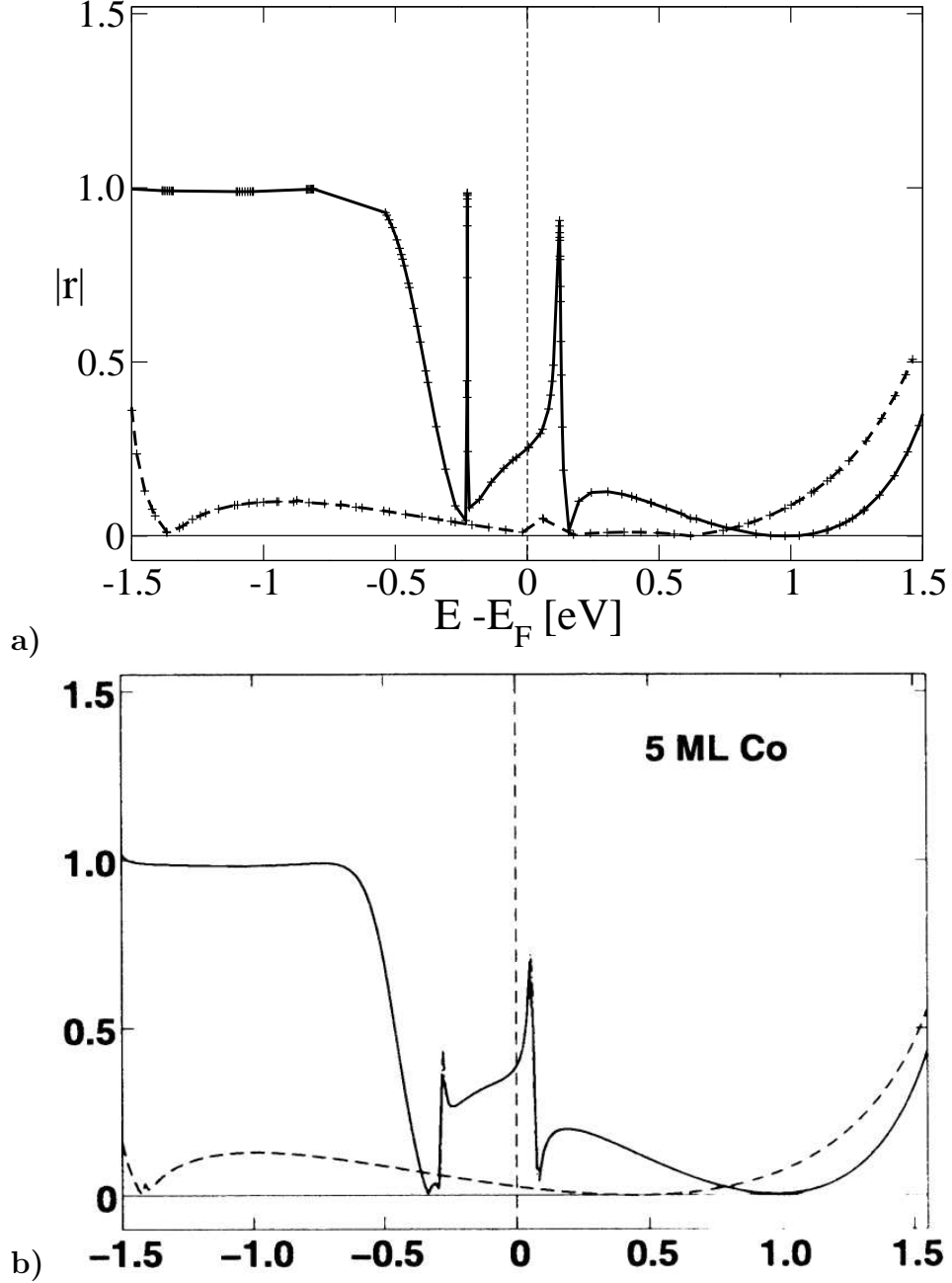


FIG. 6. The dependence of $|r|$ on $(E - E_F)$ with our new method (a) for the majority (dashed line) and minority (solid line) Cu electrons through 5 ML of Co(100) at $\mathbf{k}_{\parallel} = 0$ in comparison with Wildberger (b) (see Fig. 8.5, p.152 in [12]); the axes are the same for both figures.

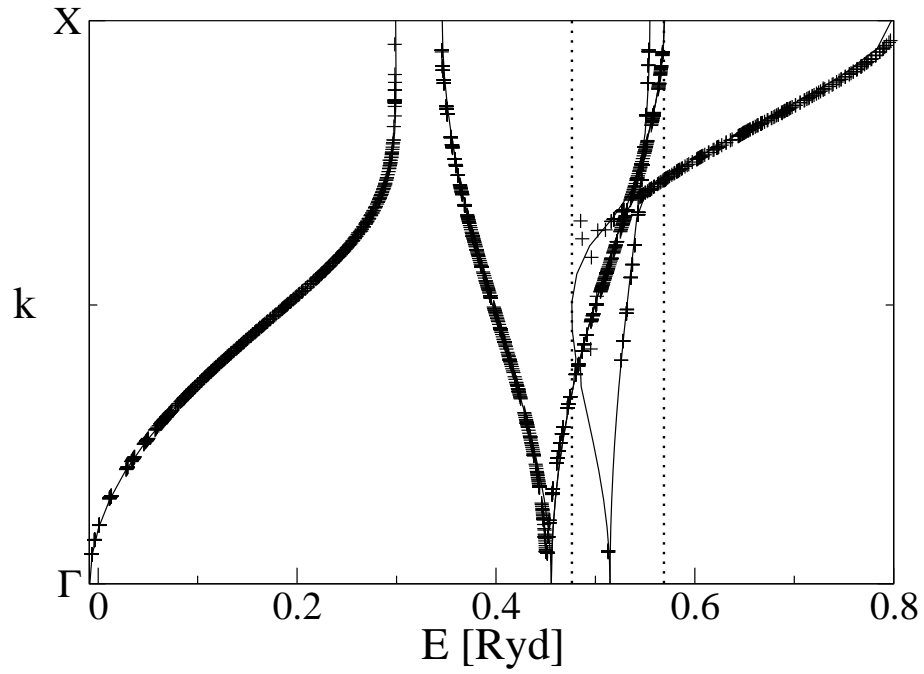


FIG. 7. Band structure of fcc Cu along ΓX from a Cu bulk calculation (solid line) and indirectly from the superlattice Cu/Co (001) calculation (cross).